OL Organic Letters

pubs.acs.org/OrgLett Letter

Combining NMR-Based Metabolic Profiling and Genome Mining for the Accelerated Discovery of Archangiumide, an Allenic Macrolide from the Myxobacterium *Archangium violaceum* SDU8

Jia-Qi Hu,[⊥] Jing-Jing Wang,[⊥] Yue-Lan Li, Li Zhuo, Ai Zhang, Hai-Yan Sui, Xiao-Ju Li, Tao Shen, Yizhen Yin, Zhi-Hong Wu, Wei Hu, Yue-Zhong Li,* and Changsheng Wu*

Cite This: *Org. Lett.* 2021, 23, 2114–2119 Read Online

ACCESS | Metrics & More | Article Recommendations | Supporting Information

ABSTRACT: An unprecedented 19-membered allenic macrolide archangiumide (**1**) was discovered from the myxobacterium *Archangium violaceum* SDU8 by integrating NMR-based metabolic profiling and genome mining. Its biosynthesis pathway was proposed based on the architectural analysis of the encoding *trans*-AT PKS genes and validated by isotope labeling. The methodology of combing 2D NMR-based metabolic profiling and bioinformatics-aided structure prediction, as exemplified by this study, is anticipated to improve discovery efficiency of a broader range of microbial "dark matter".

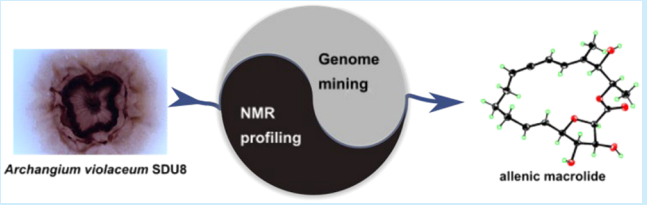

The disparity between the number of biosynthetic gene clusters (BGCs) harbored by microbes and the high rates of rediscovery necessitates new discovery pipelines. In recent years, the methodology of combining metabolomics and genomics has particularly gained favor in terms of mapping the chemical diversity of microbial natural products (NPs). Comparatively, MS-based metabolomics has much more popularity over NMR-based metabolomics in the field of microbial NPs research. Different platforms based on MS technology have been well established to correlate BGC to the encoded chemotype for the bioprospecting of microbes, such as metabologenomics,[1] peptidogenomics,[2] and glycogenomics.[3] We previously explored combining 1D ^{1}H NMR metabolic profiling and bioinformatics-aided structure elucidation to streamline the characterization of a family of novel *C*-glycosylpyranonaphthoquinones from *Streptomyces* sp. MBT76.[4] Morgan *et al.* recently combined genome mining and ^{15}N NMR based metabolomics for the targeted isolation of the piperazic acid containing peptides incarnatapeptins from *Streptomyces incarnatus* NRRL 8089.[5] These two examples indicated that NMR-based metabolomics could presumably be a complement to MS-based metabolomics with respect to linking the genotype and chemotype and, thus, elevate the probability of finding new entities. In principle, bioinformatics analysis of BGCs can predict the complete and/or partial structures of microbial NPs,[6] and the resultant chemical information can be fingerprinted by the 2D NMR-based profiling of microbial crude extracts to guide the targeted isolation and identification.[7] We reasoned that the NMR-mediated hyphenation of genomics and metabolomics is particularly applicable for the modular type I polyketide synthetase (PKS) biosynthetic system as the colinearity rule permits reliable structural predictions.[8,9]

During our continuing efforts to isolate novel myxobacterial species from diverse ecological niches, a library of ∼1000 myxobacterial strains has been set up, forming the basis for our search of the novel microbial chemistry. A myxobacterium *Archangium violaceum* SDU8 produced comparatively more compounds than its counterparts during our preliminary screening of 40 randomly selected myxobacterial strains by HPLC−UV profiling, indicating SDU8 was a prolific producer of secondary metabolites under our laboratory cultivation environment. To maximally avoid the chemical redundancy, SDU8 was first genome sequenced using the combination of Nanopore and Illumina technologies, and the assembled genome sequence was submitted to antiSMASH[10] analysis. Most of the detected 42 BGCs across disparate categories showed low or even no similarity to known BGCs, further indicating SDU8 was a promising strain for the discovery of new chemistry. Among these, a distinct *trans*-AT PKS gene cluster *arc* that likely governed the production of a macrolide was particularly interesting to us, as many *trans*-AT PKS-derived macrolides encompass distinctive architectures and/or pronounced bioactivities.[11] The continuous 53.3 kb DNA sequence of *arc* harbored 15 open reading frames that

Received: January 23, 2021
Published: March 10, 2021

https://dx.doi.org/10.1021/acs.orglett.1c00265
Org. Lett. 2021, 23, 2114–2119

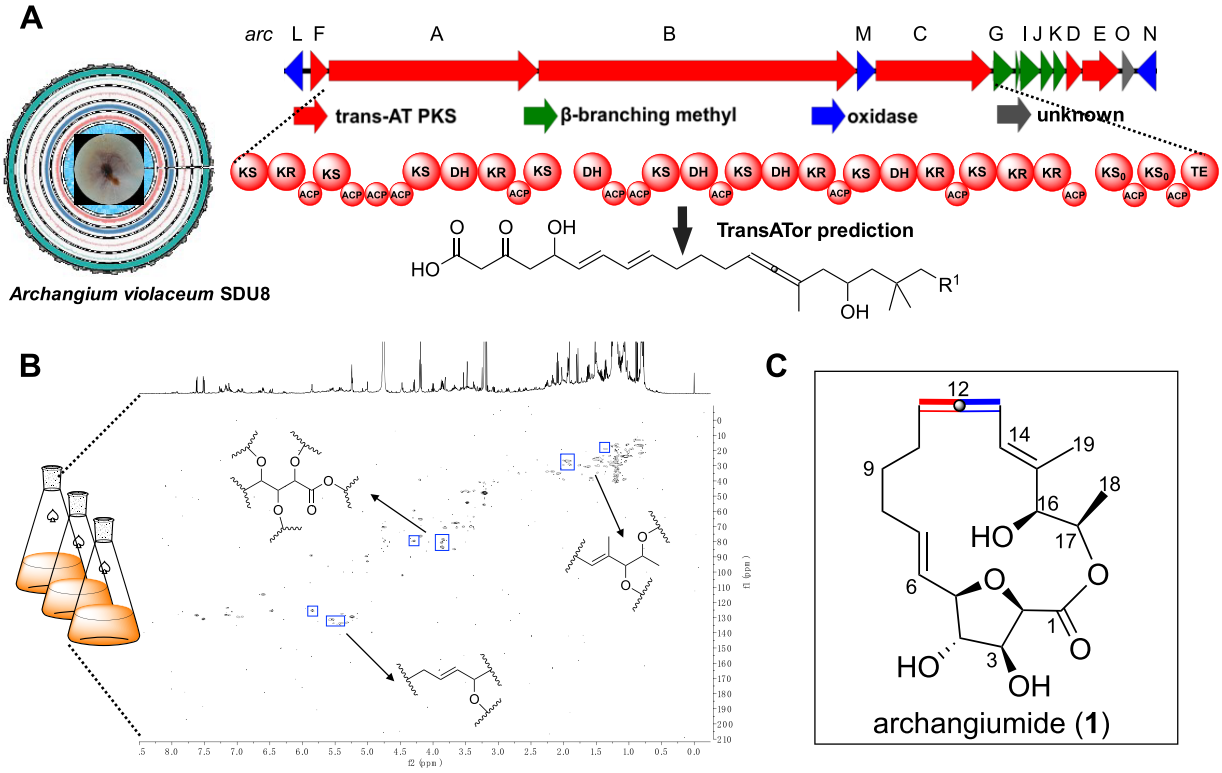

Figure 1. Joint strength of genome mining and 2D NMR-based metabolic profiling for the targeted discovery of archangiumide. (A) Genome mining of *A. violaceum* SDU8 identified a *trans*-AT PKS gene cluster. TransATor analysis of the central PKS genes allowed the prediction of the approximate structure of the encoded product. (B) 2D NMR-based metabolic profiling of SDU8 metabolome enabled the identification of fragments indicative of polyketidic macrolide. (C) Structure of archangiumide (**1**).

putatively encoded three PKSs lacking integral AT domains, two *trans*-ATs, a *β*-branching cassette, three oxidase genes, and others (Figure 1A and Table S1). AntiSMASH analysis revealed low sequence homology of *arc* to known BGCs and thus indicated the products orchestrated by *arc* could be novel. Piel et al. developed TransATor, a web-based online tool that allows de novo structural predictions for *trans*-AT PKS-derived polyketides.[12] We subjected the concatenated amino acid sequences of the three core polyketide synthases ArcA, ArcB, and ArcC to TransATor analysis, and the predicted structure contained not only the common polyketidic functionalities such as double bonds, secondary hydroxyl, vinylous methyl but also a rare allene, which was actually unprecedented in the family of polyketidic macrolides. These bioinformatic predictions compelled us to identify the products encoded by the *arc* gene cluster.

Given the BGC of interest, one of the key issues was how to efficiently characterize its chemical output(s), which is actually quite common in the field of genome mining. We explored the NMR-based metabolic profiling for the inspection of BGCs expression because NMR affords an advantage over MS in terms of unbiased detection and objective reflection of quantity ratio of all the metabolites contained in a mixture.[13] For this, SDU8 was grown in VY/2 liquid medium for 7 days, and the secreted metabolites in the culture broth were extracted by HP-20 resin and ethyl acetate (EtOAc), respectively. The following ^{1}H NMR based metabolic profiling confirmed the evidently higher complexity of HP-20 extraction compared to that of EtOAc (Figure S1). In consideration that the macrolides are normally well dissolved in EtOAc, we inferred that the EtOAc extraction method was favorable for the concentration of the potential macrolides orchestrated by *arc* gene cluster and avoided the interferents like culture medium ingredients that would be easily bonded by HP-20 resin. Therefore, EtOAc metabolome was further subjected to 2D NMR profiling, including COSY, HSQC, and HMBC (Figure S2−S4), to gain deeper insight into the expression of *arc*. Gerwick et al. recently developed a novel computational tool, the HSQC-based SMART 2.0, for the rapid characterization of macrolides in microbial crude extract.[14] We applied the SMART 2.0 tool to the HSQC spectrum of SDU8 EtOAc metabolome, and the retrieved top 12 hits suggested that macrolides were contained within (Figure S5). With the aid of HMBC and COSY spectra, we were able to identify the partial structures typical of macrolide-class natural products, corresponding to the structural prediction by TransATor (Figure 1B). Similarly, Buedenbender et al. used HSQC-TOCOSY fingerprinting to identify the characteristic structural fragments typical of macrolides at the complex metabolome level, which facilitated the dereplication of known macrolide elaiophylin[15] and also the discovery of new molecule herbimycin G.[16] Because *arc* happened to be the solely BGC that tends to specify macrolide(s) on SDU8 genome, we tentatively correlated *arc* BGC (genotype) with the 2D NMR-resolved structural features (chemotype) in the complex mixture.

NMR-guided repeated chromatographic fractionation of the up-scaled fermentation (20 L) of SDU8 led to the isolation of compound **1** (20.5 mg, Figure 1C), as a white needle crystal. HRESIMS established its molecular formula $C_{19}H_{26}O_6$ from $[M + H]^+$ peak at m/z 351.1797 (calculated for $C_{19}H_{27}O_6$), in accordance with the 19 carbon atoms counted from the ^{13}C NMR spectrum measured in DMSO-d_6. Sixteen out of the 19

https://dx.doi.org/10.1021/acs.orglett.1c00265
Org. Lett. 2021, 23, 2114−2119

carbons in the ^{13}C NMR spectrum were unambiguously assigned by HSQC as one quaternary carbonyl at δ_C 170.0, four olefinic carbons at δ_C 124.0−136.0 making up two double bonds, six oxygenated methines at δ_C 69.8−83.0, five aliphatic carbons consisting of three methylenes, and two methyls (Table 1). The connectivity of these 16 carbons were joined by

Table 1. NMR Data Assignment of Archangiumide (1)

position	δ_C, type	δ_H, mult (J, Hz)
1	170.0, C	
2	79.0, CH	4.25, d (8.5)
3	76.1, CH	4.14, td (8.0, 4.5)
4	78.0, CH	3.81, m
5	82.9, CH	3.83, m
6	131.9, CH	5.54, dd (15.5, 7.5)
7	132.6, CH	5.39, ddd (15.5 10.5, 4.0)
8	29.4, CH2	2.20, m; 2.02, m
9	26.0, CH2	1.50, m; 1.43, m
10	26.3, CH2	2.00, m; 1.94, m
11	90.1, CH	5.17, m
12	208.3, C	
13	89.9, CH	6.02, m
14	124.0, CH	5.83, d (11.5)
15	135.9, C	
16	79.6, CH	3.85, dd (6.0, 4.5)
17	69.8, CH	4.67, m
18	18.0, CH3	1.23, d (6.0)
19	10.1, CH3	1.53, s

the extensive interpretation of HMBC and COSY spectra (Figure S6). The tetrahydrofuran-3,4-diol ring was joined by the key HMBC correlations from H-2 (δ_H 4.25) to the three oxygenated methines C-3, C-4, and C-5, and the macrolide ester bonding was identified on the basis of the key HMBC correlation from H-17 to C-1 (δ_C 170.0). The linkage of the remaining three carbons at δ_C 208.3 (C-12), 90.1 (C-11), and 89.9 (C-13) was initially obscure, as the chemical shift at δ_C 208.3 was misleading and typical of ketocarbonyl. After a purely NMR approach was unsuccessful, the bioinformatics prediction of allene group by TransATor analysis compelled us to speculate C-11−C-13 making up an allene, which was indeed corroborated by a set of key HMBC correlations such as H-10, H-11, H-13, and H-14 to C-12. The ^1H and/or ^{13}C chemical shifts at C-11, C-12, and C-13 of **1** were consistent with the allene group found in crassostreaxanthins[17] and pseudoxylallemycins.[18] The addition of allene into the planar structure of **1** matched the constraints of six oxygen atoms and seven unsaturation suggested by the chemical formula. The geometry of the double bond $\Delta^{6,7}$ was identified as *E* based on the large coupling constant of 15.5 Hz. The key NOESY correlation observed between H_3-19 and H-13 also determined the *E* configuration of $\Delta^{14,15}$ (Figure S7). The absolute configuration of **1**, via 2*R*, 3*S*, 4*S*, 5*R*, 16*S*, 17*R*, was determined by single-crystal X-ray diffraction analysis (Figure 2) of pure crystals obtained by slow evaporation in methanol [Flack parameter of 0.01(8)]. The conformation observed in the crystal structure of **1** was compatible with all of the measurable coupling constants and the observed key NOESY correlations, indicating that the crystal structure was representative of the preferred conformation in solution. Taken together, compound **1** was deciphered as a novel 19-membered macrocyclic lactone featured with a rare allenic group, and we dubbed it archangiumide.

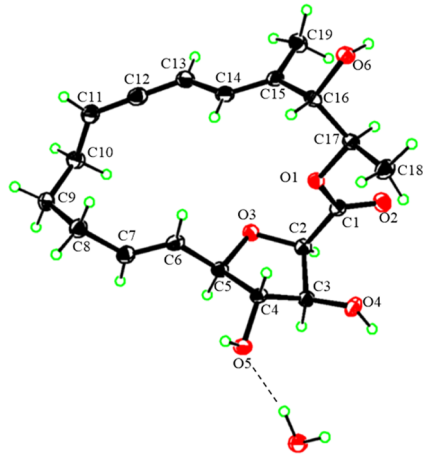

Figure 2. ORTEP diagram of the crystal structure of archangiumide. One molecule of water was cocrystallized with archangiumide by forming a hydrogen bond at 4-OH. The absolute configurations of the six chiral centers of archangiumide are 2*R*, 3*S*, 4*S*, 5*R*, 16*S*, and 17*R*.

Although allene is found in a number (~160) of natural products,[19] like cepacin,[20] puna'auic acid,[21] panacene,[22] etc., the existence of an allene group in the superfamily of macrolide was unprecedented. In terms of bioactivities, archangiumide did not show effects during the assays of anticancer (liver carcinoma cell line HepG2, breast cancer cell line MCF-7, and hepatocyte cell line HL-7702), antibacterial (*Staphylococcus aureus*, *Bacillus subtilis*, *Escherichia coli*), antifungal (*Candida albicans*), antioxidant (DPPH radical-scavenging), and anti-inflammatory effects (LPS-induced NO production in adherent cells). More extensive experiments are still needed to assess the biological function(s) of archangiumide.

On the basis of the detailed sequence analysis of the central PKS and other genes in the *arc* cluster, we proposed the biosynthetic pathway for archangiumide (Figure 3). Phylogenetic analysis of two AT-like enzymes identified ArcE as an AT with specificity for malonyl-CoA, whereas ArcD is an acyl hydrolase (Figure S8). The assembly of archangiumide starts with the loading of acetal-CoA by the free-standing ACP ArcF, followed by the consecutive extension of eight C2 units by the modules 1−8 in ArcA and ArcB. The KS domain alignment found the two KS_0 domains in ArcC are nonelongating modules (modules 9 and 10), since they lack the requisite His residue in the catalytic pocket (Figure S9). The ubiquitous presence of nonelongating modules is one of the idiosyncrasies of *trans*-AT PKS.[23] Except for a few deviations, the module architecture in ArcA and ArcB is congruent with the crystallography-confirmed structure of archangiumide, including the stereochemistry at positions C-3, C-6, and C-17 as predicted by bioinformatic analysis of KR domains[24] (Table S3 and Figure S10). However, a KR domain is missing in modules 4 and 5, and the formation of a single bond between C-8 and C-9 is also unexpected, since module 5 lacks an enoyl-reductase domain that normally performs the reduction. Such missing domains are another common peculiarity of *trans*-AT PKSs.[25−27] The *β*-branching cassette *arc*G-K is responsible for the installation of the *β*-branched methyl (C-19) and the formation of the double bond Δ.[14,15] The post-PKS route to **1** probably involves the epoxidation of the double bond C-4/C-5 by the oxidase ArcM and hydroxylation at the C-3 executed by

https://dx.doi.org/10.1021/acs.orglett.1c00265
Org. Lett. 2021, 23, 2114−2119

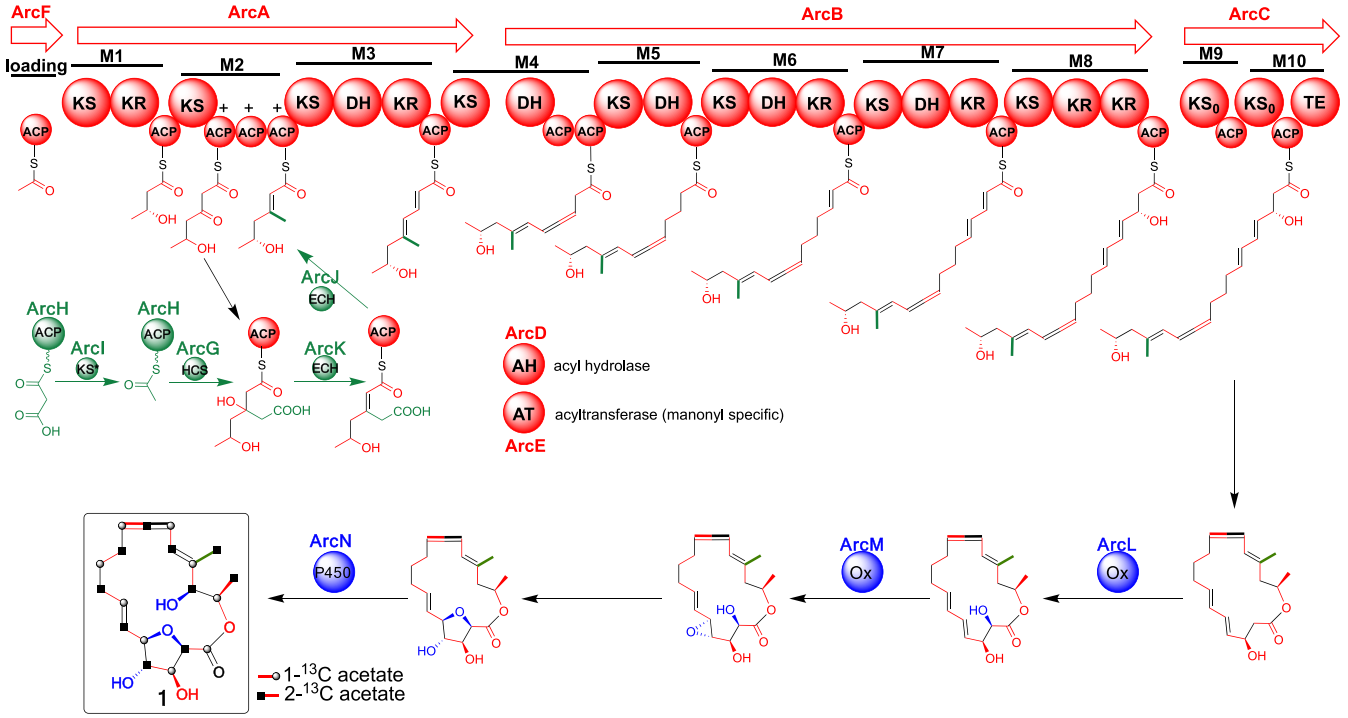

Figure 3. Model for the biosynthesis of archangiumide (**1**). The three consecutive ACP domains in module 2 of ArcA containing the conserved Trp residue recognized by the *β*-branching methylating cassette are indicated with "+" (Figure S11).[11] Domain abbreviations: ACP, acyl carrier protein; KS, ketosynthase; KS_0, nonelongating KS; KS*, KS-like enzyme; AT, *trans*-acyltransferase; AH, acyl hydrolase; KR, ketoreductase; DH, dehydratase; ECH, enoyl-CoA hydratase; HCS, hydroxymethylglutaryl-CoA synthase; P450, cytochrome P450; Ox, oxidase; TE, thioesterase. The proposed biosynthesis pathway of **1** was probed with [1-^{13}C] and [2-^{13}C] labeled sodium acetate, as boxed.

the P450 monooxygenase ArcN, followed by an intramolecular nucleophilic substitution to generate the dihydroxyfuran. The proposed online PKS assembly line, including the *β*-branching methylation, *α*, *β*-dehydration, and ketone reduction, was validated by the isotope labeling experiments by feeding with 1-^{13}C and 2-^{13}C sodium acetate, respectively (Figure S12). While the typical *α*, *β*-dehydration catalyzed by the single DH domain in ArcA gives rise to the double bond located between the incorporated acetate units at C-12/C-13, the isotope labeling experiments implied that the atypical unsaturation at C-11/C-12 is derived from *β*, *γ*-dehydration catalyzed by the first DH domain in ArcB instead of the standard *α*, *β*-pattern. Actually, the DH domain-catalyzed *β*, *γ*-dehydration or double-bond shift is not uncommon in the *trans*-AT PKS systems, such as in the biosynthesis pathway of rhizoxin[28] and corallopyronin A.[29] Future biochemistry and/or molecular biology work is needed to confirm the online PKS-catalyzed formation of allene during archangiumide biosynthesis, which is a new enzymology that could be potentially exploited to succinctly prepare the allenic reagents that are frequently used in the field of organic synthesis.[30]

The unambiguous structural determination and elucidation of the biosynthetic pathway for archangiumide demonstrated that 2D NMR-based fingerprinting had the capacity to bridge the gap between the *arc* genotype with the corresponding chemotype in the highly complex metabolome of SDU8. We were further interested if archangiumide could be discovered through an MS-based approach, since it represents a mainstay for microbial NPs research.[31] Indeed, the molecular feature *m*/*z* 351 for archangiumide was clearly exhibited in LC−MS profiling. However, it seemed difficult for MS to correlate the interested *arc* BGC with *m*/*z* 351 at a crude extract level to guide the targeted discovery of archangiumide because the peak for archangiumide was not prominent in total ion chromatography (TIC) of SDU8 metabolome (Figure S13). Meanwhile, it was also noteworthy that the relatively high yield of archangiumide (∼1 mg/L) was favorable for its detection in crude mixture by NMR, whereas the potential congener produced in low amount might be missed by NMR-directed isolation due to the intrinsic low sensitivity of NMR than MS.

In summary, we integrated the genome mining and 2D NMR based metabolic profiling into the investigation of a myxobacterium, which led to the rapid characterization of archangiumide, a novel 19-membered macrolide featuring an allene functionality and a tetrahydrofuran-3,4-diol ring. Although the biological relevance of archangiumide is unclear at this moment, its novel chemical topology underscores the effectiveness of the combination of NMR-based metabolic profiling and genome mining for the accelerated discovery of novel microbial NPs. What is needed is to develop a reliable computational tool for the simultaneous analysis of microbial genomes and metabolomes data to speed up the discovery process of a broader diversity of chemical scaffolds in a high-throughput manner. A quick way to achieve this is presumably to merge the existing algorithms[32] (e.g., antiSMASH,[10] PRISM,[8] etc.) for bioinformatics-aided structure prediction and automated NMR data analysis (e.g., DP4-AI,[33] Mix-ONat[34]) at the microbial crude extract level.[35] Moreover, it is tempting to join the tripartite strength of NMR-based metabolomics, MS-based metabolomics, and genomics for the maximal excavation of microbial "dark matter" in the future.

https://dx.doi.org/10.1021/acs.orglett.1c00265
Org. Lett. 2021, 23, 2114−2119

■ ASSOCIATED CONTENT

Supporting Information

The Supporting Information is available free of charge at https://pubs.acs.org/doi/10.1021/acs.orglett.1c00265.(PDF)

Full experimental details, biosynthetic gene cluster gene annotations, X-ray crystallographic data, prediction of stereochemistry of reduced carbon, the comparison of extraction methods, sequence alignment of KS, KR, ACP domains, and 1D, 2D, and ^{13}C isotope-labeling NMR spectra (PDF)

(PDF)

Accession Codes

CCDC 2058107 contains the supplementary crystallographic data for this paper. These data can be obtained free of charge via www.ccdc.cam.ac.uk/data_request/cif, or by emailing data_request@ccdc.cam.ac.uk, or by contacting The Cambridge Crystallographic Data Centre, 12 Union Road, Cambridge CB2 1EZ, UK; fax: +44 1223 336033.

■ AUTHOR INFORMATION

Corresponding Authors

Changsheng Wu − *State Key Laboratory of Microbial Technology, Institute of Microbial Technology, Shandong University, 266237 Qingdao, P.R. China;* orcid.org/0000-0003-1310-0089; Phone: (+86) 532-58631538; Email: wuchangsheng@sdu.edu.cn

Yue-Zhong Li − *State Key Laboratory of Microbial Technology, Institute of Microbial Technology, Shandong University, 266237 Qingdao, P.R. China;* orcid.org/0000-0001-8336-6638; Phone: (+86) 532 58631539; Email: lilab@sdu.edu.cn; Fax: (+86) 532 58631539

Authors

Jia-Qi Hu − *State Key Laboratory of Microbial Technology, Institute of Microbial Technology, Shandong University, 266237 Qingdao, P.R. China*

Jing-Jing Wang − *State Key Laboratory of Microbial Technology, Institute of Microbial Technology, Shandong University, 266237 Qingdao, P.R. China*

Yue-Lan Li − *State Key Laboratory of Microbial Technology, Institute of Microbial Technology, Shandong University, 266237 Qingdao, P.R. China*

Li Zhuo − *State Key Laboratory of Microbial Technology, Institute of Microbial Technology, Shandong University, 266237 Qingdao, P.R. China*

Ai Zhang − *Fetal Medicine Center, Qingdao Women and Children's Hospital, Qingdao University, 266071 Qingdao, P.R. China*

Hai-Yan Sui − *State Key Laboratory of Microbial Technology, Institute of Microbial Technology, Shandong University, 266237 Qingdao, P.R. China*

Xiao-Ju Li − *State Key Laboratory of Microbial Technology, Institute of Microbial Technology, Shandong University, 266237 Qingdao, P.R. China*

Tao Shen − *Key Lab of Chemical Biology (MOE), School of Pharmaceutical Sciences, Shandong University, 250100 Jinan, PR China*

Yizhen Yin − *State Key Laboratory of Microbial Technology, Institute of Microbial Technology, Shandong University, 266237 Qingdao, P.R. China*

Zhi-Hong Wu − *State Key Laboratory of Microbial Technology, Institute of Microbial Technology, Shandong University, 266237 Qingdao, P.R. China*

Wei Hu − *State Key Laboratory of Microbial Technology, Institute of Microbial Technology, Shandong University, 266237 Qingdao, P.R. China*

Complete contact information is available at: https://pubs.acs.org/10.1021/acs.orglett.1c00265

Author Contributions

[⊥]J.-Q.H. and J.-J.W. contributed equally to this work.

Notes

The authors declare no competing financial interest.

■ ACKNOWLEDGMENTS

This work was financially supported by the National Key Research and Development Programs of China (Nos. 2019YFA0905700, 2018YFA0900400, and 2018YFA0901704), the National Natural Science Foundation of China (NSFC) (Nos. 31900042, 81973215, 31670076, 31471183, and 41907105), and the Excellent Youth Program of Shandong Natural Science Foundation (No. ZR2020YQ62).

■ REFERENCES

(1) Goering, A. W.; McClure, R. A.; Doroghazi, J. R.; Albright, J. C.; Haverland, N. A.; Zhang, Y.; Ju, K. S.; Thomson, R. J.; Metcalf, W. W.; Kelleher, N. L. *ACS Cent. Sci.* **2016**, *2*, 99−108.

(2) Kersten, R. D.; Yang, Y. L.; Xu, Y.; Cimermancic, P.; Nam, S. J.; Fenical, W.; Fischbach, M. A.; Moore, B. S.; Dorrestein, P. C. *Nat. Chem. Biol.* **2011**, *7*, 794−802.

(3) Kersten, R. D.; Ziemert, N.; Gonzalez, D. J.; Duggan, B. M.; Nizet, V.; Dorrestein, P. C.; Moore, B. S. *Proc. Natl. Acad. Sci. U. S. A.* **2013**, *110*, E4407−E4416.

(4) Wu, C.; Du, C.; Ichinose, K.; Choi, Y. H.; Van Wezel, G. P. *J. Nat. Prod.* **2017**, *80*, 269−277.

(5) Morgan, K. D.; Williams, D. E.; Patrick, B. O.; Remigy, M.; Banuelos, C. A.; Sadar, M. D.; Ryan, K. S.; Andersen, R. J. *Org. Lett.* **2020**, *22*, 4053−4057.

(6) Tietz, J. I.; Mitchell, D. A. *Curr. Top. Med. Chem.* **2016**, *16*, 1645−1694.

(7) Wu, C.; Kim, H. K.; van Wezel, G. P.; Choi, Y. H. *Drug Discovery Today: Technol.* **2015**, *13*, 11−17.

(8) Skinnider, M. A.; Merwin, N. J.; Johnston, C. W.; Magarvey, N. A. *Nucleic Acids Res.* **2017**, *45*, W49−W54.

(9) Skinnider, M. A.; Johnston, C. W.; Gunabalasingam, M.; Merwin, N. J.; Kieliszek, A. M.; MacLellan, R. J.; Li, H.; Ranieri, M. R. M.; Webster, A. L. H.; Cao, M. P. T.; Pfeifle, A.; Spencer, N.; To, Q. H.; Wallace, D. P.; Dejong, C. A.; Magarvey, N. A. *Nat. Commun.* **2020**, *11*, 1−9.

(10) Blin, K.; Shaw, S.; Steinke, K.; Villebro, R.; Ziemert, N.; Lee, S. Y.; Medema, M. H.; Weber, T. *Nucleic Acids Res.* **2019**, *47*, W81−W87.

(11) Song, L.; Jenner, M.; Masschelein, J.; Jones, C.; Bull, M. J.; Harris, S. R.; Hartkoorn, R. C.; Vocat, A.; Romero-Canelon, I.; Coupland, P.; Webster, G.; Dunn, M.; Weiser, R.; Paisey, C.; Cole, S. T.; Parkhill, J.; Mahenthiralingam, E.; Challis, G. L. *J. Am. Chem. Soc.* **2017**, *139*, 7974−7981.

(12) Helfrich, E. J. N.; Ueoka, R.; Dolev, A.; Rust, M.; Meoded, R. A.; Bhushan, A.; Califano, G.; Costa, R.; Gugger, M.; Steinbeck, C.; Moreno, P.; Piel, J. *Nat. Chem. Biol.* **2019**, *15*, 813−821.

(13) Pan, Z.; Raftery, D. *Anal. Bioanal. Chem.* **2007**, *387*, 525−527.

(14) Reher, R.; Kim, H. W.; Zhang, C.; Mao, H. H.; Wang, M.; Nothias, L. F.; Caraballo-Rodriguez, A. M.; Glukhov, E.; Teke, B.; Leao, T.; Alexander, K. L.; Duggan, B. M.; Van Everbroeck, E. L.;

Dorrestein, P. C.; Cottrell, G. W.; Gerwick, W. H. *J. Am. Chem. Soc.* **2020**, *142*, 4114−4120.
(15) Buedenbender, L.; Habener, L. J.; Grkovic, T.; Kurtböke, D. I.; Duffy, S.; Avery, V. M.; Carroll, A. R. *J. Nat. Prod.* **2018**, *81*, 957−965.
(16) Buedenbender, L.; Robertson, L. P.; Lucantoni, L.; Avery, V. M.; Ke, D. I. K.; Carroll, A. R. *Mar. Drugs* **2018**, *16*, 189−199.
(17) Maoka, T.; Hashimoto, K.; Akimoto, N.; Fujiwara, Y. *J. Nat. Prod.* **2001**, *64*, 578−581.
(18) Guo, H.; Kreuzenbeck, N. B.; Otani, S.; Garcia-Altares, M.; Dahse, H. M.; Weigel, C.; Aanen, D. K.; Hertweck, C.; Poulsen, M.; Beemelmanns, C. *Org. Lett.* **2016**, *18*, 3338−3341.
(19) Hoffmann-Röder, A.; Krause, N. *Angew. Chem., Int. Ed.* **2004**, *43*, 1196−1216.
(20) Mullins, A. J.; Murray, J. A. H.; Bull, M. J.; Jenner, M.; Jones, C.; Webster, G.; Green, A. E.; Neill, D. R.; Connor, T. R.; Parkhill, J.; Challis, G. L.; Mahenthiralingam, E. *Nat. Microbiol.* **2019**, *4*, 996−1005.
(21) Roulland, E.; Solanki, H.; Calabro, K.; Zubia, M.; Genta-Jouve, G.; Thomas, O. P. *Org. Lett.* **2018**, *20*, 2311−2314.
(22) Alnafta, N.; Schmidt, J. P.; Nesbitt, C. L.; McErlean, C. S. P. *Org. Lett.* **2016**, *18*, 6520−6522.
(23) Helfrich, E. J. N.; Piel, J. *Nat. Prod. Rep.* **2016**, *33*, 231−316.
(24) Kim, M. C.; Machado, H.; Jang, K. H.; Trzoss, L.; Jensen, P. R.; Fenical, W. *J. Am. Chem. Soc.* **2018**, *140*, 10775−10784.
(25) Piel, J. *Nat. Prod. Rep.* **2010**, *27*, 996−1047.
(26) Helfrich, E. J. N.; Piel, J. *Nat. Prod. Rep.* **2016**, *33*, 231−316.
(27) Helfrich, E. J. N.; Ueoka, R.; Dolev, A.; Rust, M.; Meoded, R. A.; Bhushan, A.; Califano, G.; Costa, R.; Gugger, M.; Steinbeck, C.; Moreno, P.; Piel, J. *Nat. Chem. Biol.* **2019**, *15*, 813−821.
(28) Kusebauch, B.; Busch, B.; Scherlach, K.; Roth, M.; Hertweck, C. *Angew. Chem., Int. Ed.* **2010**, *49*, 1460−1464.
(29) Erol, Ö.; Schäberle, T. F.; Schmitz, A.; Rachid, S.; Gurgui, C.; El Omari, M.; Lohr, F.; Kehraus, S.; Piel, J.; Müller, R.; Königd, G. M. *ChemBioChem* **2010**, *11*, 1253−1265.
(30) Adamson, N. J.; Jeddi, H.; Malcolmson, S. J. *J. Am. Chem. Soc.* **2019**, *141*, 8574−8583.
(31) van der Hooft, J. J. J.; Mohimani, H.; Bauermeister, A.; Dorrestein, P. C.; Duncan, K. R.; Medema, M. H. *Chem. Soc. Rev.* **2020**, *49*, 3297−3314.
(32) Blin, K.; Kim, H. U.; Medema, M. H.; Weber, T. *Briefings Bioinf.* **2019**, *20*, 1103−1113.
(33) Howarth, A.; Ermanis, K.; Goodman, J. M. *Chem. Sci.* **2020**, *11*, 4351−4359.
(34) Bruguière, A.; Derbre, S.; Dietsch, J.; Leguy, J.; Rahier, V.; Pottier, Q.; Brea'rd, D.; Suor-Cherer, S.; Viault, G.; Ray, A.-M. L.; Saubion, F.; Richomme, P. *Anal. Chem.* **2020**, *92*, 8793−8801.
(35) Buedenbender, L.; Habener, L. J.; Grkovic, T.; Kurtböke, D. I.; Duffy, S.; Avery, V. M.; Carroll, A. R. *J. Nat. Prod.* **2018**, *81*, 957−965.

■ NOTE ADDED AFTER ASAP PUBLICATION

Figure 1 was corrected on March 12, 2021.

https://dx.doi.org/10.1021/acs.orglett.1c00265
Org. Lett. 2021, 23, 2114−2119